Article

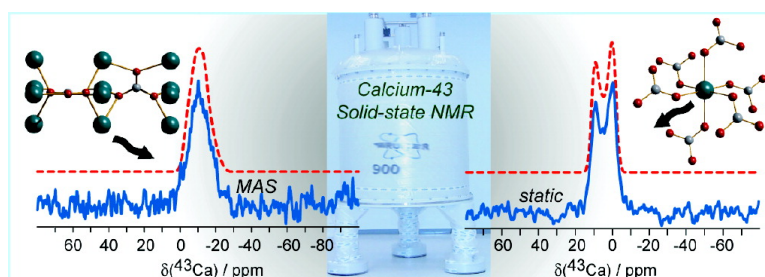# Calcium-43 Chemical Shift Tensors as Probes of Calcium Binding Environments. Insight into the Structure of the Vaterite CaCO Polymorph by Ca Solid-State NMR Spectroscopy

David L. Bryce, Elijah B. Bultz, and Dominic Aebi

More About This Article

Additional resources and features associated with this article are available within the HTML version:

- Supporting Information
- Links to the 1 articles that cite this article, as of the time of this article download
- Access to high resolution figures
- Links to articles and content related to this article
- Copyright permission to reproduce figures and/or text from this article

View the Full Text HTML

Calcium-43 Chemical Shift Tensors as Probes of Calcium Binding Environments. Insight into the Structure of the Vaterite CaCO$_3$ Polymorph by ^{43}Ca Solid-State NMR Spectroscopy

David L. Bryce,* Elijah B. Bultz, and Dominic Aebi

Department of Chemistry and Centre for Catalysis Research and Innovation, University of Ottawa, Ottawa, Ontario K1N 6N5, Canada

Received March 7, 2008; Revised Manuscript Received May 6, 2008; E-mail: dbryce@uottawa.ca

Abstract: Natural-abundance ^{43}Ca solid-state NMR spectroscopy at 21.1 T and gauge-including projector-augmented-wave (GIPAW) DFT calculations are developed as tools to provide insight into calcium binding environments, with special emphasis on the calcium chemical shift (CS) tensor. The first complete analysis of a ^{43}Ca solid-state NMR spectrum, including the relative orientation of the CS and electric field gradient (EFG) tensors, is reported for calcite. GIPAW calculations of the ^{43}Ca CS and EFG tensors for a series of small molecules are shown to reproduce experimental trends; for example, the trend in available solid-state chemical shifts is reproduced with a correlation coefficient of 0.983. The results strongly suggest the utility of the calcium CS tensor as a novel probe of calcium binding environments in a range of calcium-containing materials. For example, for three polymorphs of CaCO$_3$ the CS tensor span ranges from 8 to 70 ppm and the symmetry around calcium is manifested differently in the CS tensor as compared with the EFG tensor. The advantages of characterizing the CS tensor are particularly evident in very high magnetic fields where the effect of calcium CS anisotropy is augmented in hertz while the effect of second-order quadrupolar broadening is often obscured for ^{43}Ca because of its small quadrupole moment. Finally, as an application of the combined experimental−theoretical approach, the solid-state structure of the vaterite polymorph of calcium carbonate is probed and we conclude that the hexagonal *P*6$_3$/*mmc* space group provides a better representation of the structure than does the orthorhombic *Pbnm* space group, thereby demonstrating the utility of ^{43}Ca solid-state NMR as a complementary tool to X-ray crystallographic methods.

Introduction

Calcium is an important element which is present in a wide range of materials and biologically important molecules,[1–6] and there is currently great interest in the further development of ^{43}Ca solid-state nuclear magnetic resonance (SSNMR) spectroscopy as a useful tool for studying such diverse systems. However, calcium-43 SSNMR has traditionally been challenging due primarily to the low natural abundance of this nucleus (0.135%). Ca-43 is quadrupolar ($I = 7/2$); however, the nuclear electric quadrupole moment is relatively small ($Q = -4.08$ fm^2).[7] The magnetogyric ratio is fairly low, thereby also contributing to difficulties in observing this nucleus ($\gamma = -1.803 \times 10^7$ rad T^{-1} s^{-1}; $\nu_0 = 33.66$ MHz at 11.75 T). For these

reasons, the literature is not extensive for this nucleus[8–20] although recent natural abundance work by Smith and co-workers[21–23] as well as some studies on isotopically enriched slags and glasses,[24–27] along with the increasing availability of very high field SSNMR spectrometers, has rekindled interest in ^{43}Ca. A particularly outstanding example reported this year by Laurencin et al. demonstrated the utility of triple-quantum

(1) Soderling, T. R.; Stull, J. T. *Chem. Rev.* **2001**, *101*, 2341–2351.

(2) Hofmann, M. P.; Gbureck, U.; Duncan, C. O.; Dover, M. S.; Barralet, J. E. *J. Biomed. Mater. Res. Part B* **2007**, *83B*, 1–8.

(3) Sato, K.; Yamaguchi, S.; Nemizu, T.; Fujita, S.; Suzuki, K.; Mori, T. *J. Ceram. Soc. Jpn.* **2007**, *115*, 370–373.

(4) Wilson, C. E.; Kruyt, M. C.; de Bruijn, J. D.; van Blitterswijk, C. A.; Oner, F. C.; Verbout, A. J.; Dhert, W. J. A. *Biomaterials* **2006**, *27*, 302–314.

(5) Diyabalanage, H. V. K.; Shrestha, R. P.; Semelsberger, T. A.; Scott, B. L.; Bowden, M. E.; Davis, B. L.; Burrell, A. K. *Angew. Chem., Int. Ed.* **2007**, *46*, 8995–8997.

(6) Vallet-Regí, M.; González-Calbet, J. M. *Prog. Solid State Chem.* **2004**, *32*, 1–31.

(7) Pyykkö, P. *Mol. Phys.* **2001**, *99*, 1617–1629.

(8) Mackenzie, K. J. D.; Smith, M. E. *Multinuclear Solid-State NMR of Inorganic Materials*; Pergamon Materials Series; Cahn, R. W., Ed.; Pergamon: Amsterdam, 2002.

(9) Smith, M. E. *Annu. Rep. Nucl. Magn. Reson. Spectrosc.* **2001**, *43*, 121–175.

(10) Bryant, R. G.; Ganapathy, S.; Kennedy, S. D. *J. Magn. Reson.* **1987**, *72*, 376–378.

(11) Dupree, R.; Howes, A. P.; Kohn, S. C. *Chem. Phys. Lett.* **1997**, *276*, 399–404.

(12) Zanni, H.; Rassem-Bertolo, R.; Masse, S.; Fernandez, L.; Nieto, P.; Bresson, B. *Magn. Reson. Imag.* **1996**, *14*, 827–831.

(13) Nieto, P.; Dron, R.; Thouvenot, R.; Zanni, H.; Brivot, F. *C. R. Acad. Sci. Paris, Série II* **1995**, *320*, 485–488.

(14) Marchand, S.; Trokiner, A.; Yakubovsky, A.; Knizhnik, A.; Eckstein, Y. *Physica C (Amsterdam, Neth.)* **2004**, *408–410*, 826–827.

(15) Trokiner, A.; Noc, L. L.; Yakubovskii, A.; Mykhalyov, K. N.; Verkhovskii, S. V. *J. Chim. Phys. Phys.−Chim. Biol.* **1994**, *91*, 862–868.

(16) Trokiner, A.; Lenoc, L.; Yakubovskii, A.; Mykhalyov, K. N.; Verkhovskii, S. V. *Z. Naturforsch.* **1994**, *49a*, 373–378.

(17) Marchand, S.; Trokiner, A.; Yakubovskii, A.; Monod, P.; Knizhnik, A.; Eckstein, Y. *C. R. Acad. Sci. Paris, Chimie/Chemistry* **2001**, *4*, 819–824.

^{43}Ca magic-angle spinning (MAS) NMR in distinguishing between the two crystallographically distinct calcium sites in hydroxyapatite.[28,29] This work also impressively showed that natural abundance ^{43}Ca$-^{1}$H rotational-echo double-resonance (REDOR) experiments are feasible, thereby opening the door to distance measurements involving calcium. Solution ^{43}Ca NMR spectroscopy is also very useful, having found applications in characterizing calcium-binding proteins,[30,31] and as reported recently by Wu and co-workers, Ca^{2+} binding to G-quartets.[32]

One of the issues which has become apparent is that, because of the small quadrupole moment of ^{43}Ca, second-order quadrupolar effects on the central transition (1/2 $\leftrightarrow$ $-$1/2) are often small and spectral features associated with such effects are often not resolved. This has been exemplified in recent studies where line widths were the only data extractable from the ^{43}Ca line shapes, rather than well-defined quadrupolar coupling constants (C_Q) and asymmetry parameters (η_Q). The issue is compounded by the high nuclear spin quantum number of ^{43}Ca, since second-order quadrupolar effects are effectively diminished relative to lower-half-integer-spin nuclei.[33] Certainly reduced second-order quadrupolar effects are very desirable in many instances, given the increased spectral resolution which can result. However, clearly some information on the quadrupolar tensor can be lost under such circumstances.

On this basis, and given that the known range of isotropic chemical shifts for calcium is sizable (about 250 ppm),[34] we suggest that calcium chemical shift (CS) tensors should be taken advantage of to provide useful complementary insights into the local calcium environment. Chemical shift tensors are intimately related to the electronic structure about the nucleus of interest.[35–37] To our knowledge, the only previous published report of calcium CS anisotropy is that of Dupree for the aragonite polymorph of calcium carbonate;[11] a CS tensor span ($\Omega = \delta_{11}-\delta_{33}$) of 57 $\pm$ 4 ppm was obtained. No information on the relative orientation
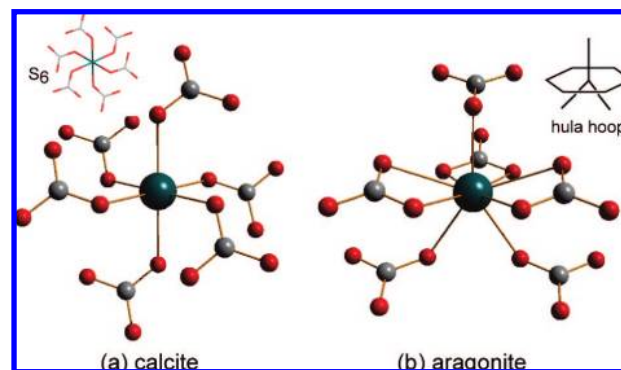

Figure 1. Calcium coordination environments in the calcite and aragonite polymorphs of CaCO$_3$. (a) Calcium is in a six-coordinate pseudo-octahedral environment of S_6 symmetry in calcite. (b) Calcium is in a nine-coordinate distorted hula-hoop environment in aragonite. Images generated using Diamond[86] and POVRay.[87]

of the CS and quadrupolar tensors was reported. Despite all of the recent advances and interest in ^{43}Ca NMR, therefore, no published literature reports describe the characterization of a calcium site in terms of the ^{43}Ca quadrupolar and CS tensor eigenvalues and the relative orientation of these tensors. Importantly, some recent conference presentations have addressed this issue,[38,39] e.g., Ellis and Lipton have reported results for ^{43}Ca-enriched calcium acetate.[39] Due to the strong current interest in the development and application of ^{43}Ca SSNMR,[25,27,28] the characterization described in the present report is timely.

All three CaCO$_3$ polymorphs (calcite, aragonite, and meta-stable vaterite; see Figures 1 and 2) have wide-ranging applications and occur naturally under various conditions.[40] For example, calcite has recently been used as a templating agent for creating intracrystalline pores in silicalite-1 crystals,[41] and vaterite deposited on biodegradable polymer foam scaffolds has been used to induce bone-like hydroxycarbonate apatite coatings.[42] Calcium carbonate has also been used recently in mixed cement compositions for bone reconstruction.[43] Naturally occurring CaCO$_3$ polymorphs are found in human gallstones,[44,45] with vaterite being found in 87% of analyzed stones in a study by Palchik and Moroz; their finding is remarkable in that the order of relative abundances of the three polymorphs in gallstones is the reverse of what is found elsewhere in nature, where calcite is the dominant form.[46] Another interesting natural occurrence of the metastable vaterite polymorph is in freshwater

(18) Padro, D.; Jennings, V.; Smith, M. E.; Hoppe, R.; Thomas, P. A.; Dupree, R. *J. Phys. Chem. B* **2002**, *106*, 13176–13185.

(19) MacKenzie, K. J. D.; Schmücker, M.; Smith, M. E.; Poplett, I. J. F.; Kemmitt, T. *Thermochim. Acta* **2000**, *363*, 181–188.

(20) Trokiner, A.; Bessière, A.; Thouvenot, R.; Hau, D.; Marko, J.; Nardello, V.; Pierlot, C.; Aubry, J.-M. *Solid State Nucl. Magn. Reson.* **2004**, *25*, 209–215.

(21) Lin, Z.; Smith, M. E.; Sowrey, F. E.; Newport, R. J. *Phys. Rev. B* **2004**, *69*, 224107.

(22) Wong, A.; Howes, A. P.; Dupree, R.; Smith, M. E. *Chem. Phys. Lett.* **2006**, *427*, 201–205.

(23) MacKenzie, K. J. D.; Smith, M. E.; Wong, A. *J. Mater. Chem.* **2007**, *17*, 5090–5096.

(24) Shimoda, K.; Tobu, Y.; Kanehashi, K.; Saito, K. *Solid State Nucl. Magn. Reson.* **2006**, *30*, 198–202.

(25) Shimoda, K.; Tobu, Y.; Shimoikeda, Y.; Nemoto, T.; Saito, K. *J. Magn. Reson.* **2007**, *186*, 156–159.

(26) Shimoda, K.; Tobu, Y.; Kanehashi, K.; Nemoto, T.; Saito, K. *Chem. Lett.* **2005**, *34*, 1588–1589.

(27) Angeli, F.; Gaillard, M.; Jollivet, P.; Charpentier, T. *Chem. Phys. Lett.* **2007**, *440*, 324–328.

(28) Laurencin, D.; Wong, A.; Hanna, J. V.; Dupree, R.; Smith, M. E. *J. Am. Chem. Soc.* **2008**, *130*, 2412–2413.

(29) Laurencin, D.; Wong, A.; Dupree, R.; Smith, M. E. *Magn. Reson. Chem.* **2008**, *46*, 347–350.

(30) Aramini, J. M.; Drakenberg, T.; Hiraoki, T.; Ke, Y.; Nitta, K.; Vogel, H. J. *Biochemistry* **1992**, *31*, 6761–6768.

(31) Aramini, J. M.; Vogel, H. J. *Biochem. Cell Biol.* **1998**, *76*, 210–222.

(32) Kwan, I. C. M.; Wong, A.; She, Y.-M.; Smith, M. E.; Wu, G. *Chem. Commun.* **2008**, 682–684.

(33) Amoureux, J. P. ; Fernandez, C. ; Granger, P. In *Multinuclear Magnetic Resonance in Liquids and Solids - Chemical Applications, NATO ASI Series C - Vol. 322*; Granger, P. ; Harris, R. K., Eds.; Kluwer Academic Publishers: Dordrecht, 1990; chapter XXII.

(34) Akitt, J. W. In *Multinuclear NMR*; Mason, J., Ed.; Plenum Press: New York, 1987; Chapter 7.

(35) Ramsey, N. F. *Molecular Beams*; Oxford University Press: London, 1956; pp 162−166, 208−213.

(36) (a) Ramsey, N. F. *Phys. Rev.* **1950**, *77*, 567. (b) Ramsey, N. F. *Phys. Rev.* **1950**, *78*, 699–703. (c) Ramsey, N. F. *Phys. Rev.* **1951**, *83*, 540–541. (d) Ramsey, N. F. *Phys. Rev.* **1952**, *86*, 243–246.

(37) Casabianca, L. B.; de Dios, A. C. *J. Chem. Phys.* **2008**, *128*, 052201.

(38) Bryce, D. L.; Adiga, S.; Aebi, D.; Chapman, B.; Lee, P. K.; Sward, G. D.; Zhang, L. Oral presentation at the NMR of Metals in Biological Systems and Materials International Symposium and Workshop, University of Delaware, June 9−10, 2007.

(39) Ellis, P. D.; Lipton, A. S. Oral presentation at the NMR of Metals in Biological Systems and Materials International Symposium and Workshop, University of Delaware, June 9−10, 2007.

(40) Brečević, L.; Kralj, D. *Croat. Chem. Acta* **2007**, *80*, 467–484.

(41) Zhu, H.; Liu, Z.; Wang, Y.; Kong, D.; Yuan, X.; Xie, Z. *Chem. Mater.* **2008**, *20*, 1134–1139.

(42) Maeda, H.; Maquet, V.; Kasuga, T.; Chen, Q. Z.; Roether, J. A.; Boccaccini, A. R. *J. Mater. Sci.: Mater. Med.* **2007**, *18*, 2269–2273.

(43) Combes, C.; Bareille, R.; Rey, C. *J. Biomed. Mater. Res., Part A* **2006**, *79*, 318–328.

(44) Sutor, D. J.; Wooley, S. E. *Science* **1968**, *159*, 1113–1114.

(45) Taylor, D. R.; Crowther, R. S.; Cozart, J. C.; Sharrock, P.; Wu, J.; Soloway, R. D. *Hepatology* **1995**, *22*, 488–496.
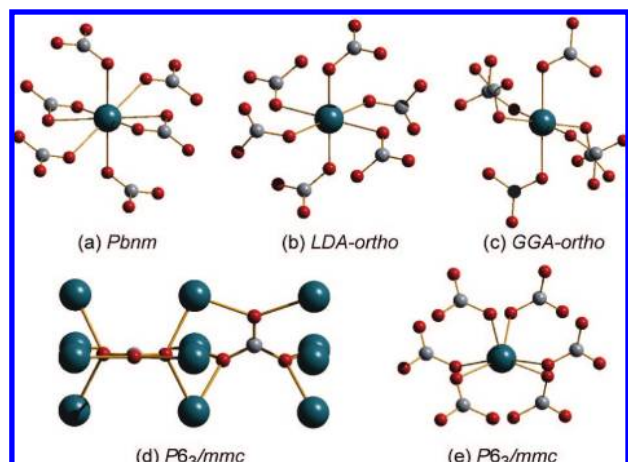
Figure 2. Structural models for the vaterite polymorph of calcium carbonate. (a) Orthorhombic *Pbnm* structure. (b) LDA-optimized orthorhombic structure. (c) GGA-optimized orthorhombic structure. (d) Two adjacent unit cells of the *P6₃/mmc* structure, with only one carbonate group per cell shown (disorder not shown). (e) Same as part d but viewed from the perspective of the coordination environment around a single calcium cation.

lackluster pearls.[47] Despite the importance of these polymorphs in nature and their varied applications, there exists in the literature a debate over the best crystallographic representation of the structure of vaterite, with hexagonal $P6_3/mmc$[48,49] and orthorhombic $Pbnm$[50] space groups having been proposed.

In this contribution, we demonstrate the general importance of calcium CS anisotropy in the interpretation of ^{43}Ca SSNMR spectra and show that the calcium CS tensor has the potential to become a useful new tool in the discrimination and characterization of calcium-containing molecules including polymorphic materials. This is achieved through a combination of ultra-high-field ($B_0 = 21.1$ T) ^{43}Ca SSNMR spectroscopy and state-of-the-art gauge-including projector-augmented-wave (GIPAW) calculations of calcium electric field gradient (EFG) and nuclear magnetic shielding tensors. The very high magnetic field allows for precise measurement of small CS anisotropies while the GIPAW method[51,52] enables accurate calculation of NMR parameters for extended ionic solids.[53] The combined experimental−theoretical protocol is developed on the calcite polymorph of $CaCO_3$ and further validated using GIPAW calculations and available experimental data for a series of calcium compounds. The protocol is then applied to provide

fresh evidence for the best crystallographic representation of the vaterite polymorph of $CaCO_3$.

Experimental and Computational Details

(a) Sample Preparation. All samples studied were natural abundance in calcium-43 (0.135%). Two different calcite samples were obtained from Aldrich and used without further purification: a 99.999% pure powder and a single-crystal optical grade sample. Additionally, calcite was prepared by precipitation (Na_2CO_3 and $CaCl_2 \cdot 2H_2O$ in water). The best spectra (i.e., those with the most well-defined second-order quadrupolar line shapes), which are reported herein, were obtained by grinding an optical grade single crystal into a fine powder. CaO powder was obtained from Aldrich and from Strem Chemical.

Vaterite was prepared according to the procedure described in ref 54. A typical synthesis was performed as follows. Glycine (6.11 g) obtained from Sigma-Aldrich was dissolved in 100 mL of distilled water, to which 10 mL of 0.5 M Na_2CO_3(aq) were added dropwise over a period of 5 min. The resulting solution was stirred at room temperature for 20 min, after which time 10 mL of 0.5 M $CaCl_2 \cdot 2H_2O$(aq) were added dropwise over a period of 10 min, with continuous stirring. Vaterite precipitates slowly from the solution, and the resulting fine white powder was filtered and air-dried. A powder X-ray pattern for the powder obtained matched the known pattern for vaterite (see Supporting Information). All samples were finely powdered with a mortar and pestle and then packed into 10 mm o.d. glass tubes or 7 mm o.d. zirconia rotors.

(b) Solid-State NMR Spectroscopy. Calcium-43 solid-state NMR spectra were obtained at frequencies of 33.66 MHz (11.75 T) and 60.59 MHz (21.1 T) using Bruker Avance and Avance II consoles. At 11.75 T, a 10 mm solenoid probe was used while at 21.1 T a 7 mm MAS probe was used. Pulse calibration and chemical shift referencing were achieved using a saturated $CaCl_2$ aqueous solution (set to 0 ppm). This saturated solution was very viscous relative to a more dilute (e.g., 2 M) solution. The 'solid' $\pi/2$ pulse lengths (scaled from the 'solution' values by a factor of $1/(I + 1/2) = 1/4$) were 1.5 μs at 21.1 T and 2.63 μs at 11.75 T. All FIDs were recorded as simple Bloch decays. Recycle delays of 1 to 60 s were used. Spectra were simulated using WSOLIDS[55] and stack plots were prepared using DMFit.[56]

(c) Quantum Chemical Calculations. Quantum chemical calculations of the calcium EFG and nuclear magnetic shielding tensors were performed using structural models for the compounds which were built from available crystallographic data.[57] The compounds studied were: CaB_6, $CaBr_2$, $CaCl_2$, CaF_2, $Ca(OH)_2$,[58] CaS, CaSe, CaH_2,[59] calcite, aragonite, vaterite, $CaMoO_4$, CaO, $CaWO_4$,[60] $CaZrO_3$,[61] and calcium formate.[62] Note that the structures

(46) Palchik, N. A.; Moroz, T. N. *J. Cryst. Growth* **2005**, *283*, 450–456.
(47) Qiao, L.; Feng, Q.-L.; Li, Z. *Cryst. Growth Des.* **2007**, *7*, 275–279.
(48) Kahmi, S. R. *Acta Crystallogr.* **1963**, *16*, 770–772.
(49) Meyer, H. J. *Z. Kristallogr.* **1969**, *128*, S183–212.
(50) Meyer, H.-J. *Angew. Chem.* **1959**, *71*, 678–679.
(51) Pickard, C. J. ; Mauri, F. In *Calculation of NMR and EPR Parameters. Theory and Applications*; Kaupp, M. ; Bühl, M. ; Malkin, V. G., Eds.; Wiley-VCH Verlag GmbH & co. KGaA: Weinheim, 2004; chapter 16.
(52) (a) Clark, S. J.; Segall, M. D.; Pickard, C. J.; Hasnip, P. J.; Probert, M. J.; Refson, K.; Payne, M. C. *Z. Krystallogr.* **2005**, *220*, 567–570. (b) Segall, M. D.; Lindan, P. J. D.; Probert, M. J.; Pickard, C. J.; Hasnip, P. J.; Clark, S. J.; Payne, M. C. *J. Phys.: Condens. Matter* **2002**, *14*, 2717–2744. (c) Pickard, C. J.; Mauri, F. *Phys. Rev. B* **2001**, *63*, 245101. (d) Profeta, M.; Mauri, F.; Pickard, C. J. *J. Am. Chem. Soc.* **2003**, *125*, 541–548.

(53) (a) Benoit, M.; Profeta, M.; Mauri, F.; Pickard, C. J.; Tuckerman, M. E. *J. Phys. Chem. B* **2005**, *109*, 6052–6060. (b) Harris, R. K.; Joyce, S. A.; Pickard, C. J.; Cadars, S.; Emsley, L. *Phys. Chem. Chem. Phys.* **2006**, *8*, 137–143. (c) Mifsud, N.; Elena, B.; Pickard, C. J.; Lesage, A.; Emsley, L. *Phys. Chem. Chem. Phys.* **2006**, *8*, 3418–3422. (d) Zwanziger, J. W.; Werner-Zwanziger, U.; Zanotto, E. D.; Rotari, E.; Glebova, L. N.; Glebov, L. B.; Schneider, J. F. *J. Appl. Phys.* **2006**, *99*, 083511. (e) Zwanziger, J. W.; Shaw, J. L.; Werner-Zwanziger, U.; Aitken, B. G. *J. Phys. Chem. B* **2006**, *110*, 20123–20128.
(54) Shivkumara, C.; Singh, P.; Gupta, A.; Hegde, M. S. *Mater. Res. Bull.* **2006**, *41*, 1455–1460.
(55) Eichele, K.; Wasylishen, R. E. WSOLIDS1: WSOLIDS NMR Simulation Package, Version 1.17.30; Universität Tübingen, Tübingen, 2001.
(56) Massiot, D.; Fayon, F.; Capron, M.; King, I.; Le Calvé, S.; Alonso, B.; Durand, J-O.; Bujoli, B.; Gan, Z.; Hoatson, G. *Magn. Reson. Chem.* **2002**, *40*, 70–76.
(57) Wyckoff, R. W. G. *Crystal Structures*, 2nd edition; Wiley: New York, 1963.
(58) Busing, W. R.; Levy, H. A. *J. Chem. Phys.* **1957**, *26*, 563–568.
(59) Bergsma, J.; Loopstra, B. O. *Acta Crystallogr.* **1962**, *15*, 92–93.
(60) (a) Zalkin, A.; Templeton, D. H. *J. Chem. Phys.* **1964**, *40*, 501–504. (b) Kay, M. I.; Frazer, B. C.; Almodovar, I. *J. Chem. Phys.* **1964**, *40*, 504–506.

for the three molecules containing hydrogen atoms are based on neutron diffraction data. In the case of the vaterite polymorph of $CaCO_3$, experimental orthorhombic *Pbnm*[50] and hexagonal *P6₃/mmc*[48,49] structures, as well as two DFT-optimized structures reported by Medeiros et al.[63] were used (Figure 2). These latter two structures are based on the proposed experimental orthorhombic structure and we label them as LDA-ortho and GGA-ortho. Since the hexagonal structure exhibits static disorder of the carbonate ions, calculations were run using a supercell constructed from two unit cells in which the carbonate ion orientations in adjacent cells were chosen to be different from each other (see Figure 2d). For this small two-cell model, computed results for various relative orientations of the carbonate ions were identical to each other. To model the effect of longer-range disorder by constructing a larger supercell exceeded our current computational resources given that the number of possible supercells to test will increase geometrically with supercell size.

Gauge-including projector-augmented wave (GIPAW) DFT calculations were carried out using the CASTEP NMR package (version 4.1).[52] The calcium on-the-fly pseudopotential file was obtained directly from Accelrys Inc. (San Diego, CA). All calculations used the generalized gradient approximation (GGA) and the PBE functional.[64] The dependence of calculated NMR interaction tensors on the plane-wave basis set cutoff energy was explored; all final results herein were obtained with a cutoff energy of 610 eV. The default Materials Studio "medium" setting was used to automatically set the number of Monkhorst-Pack grid k-points sampling the Brillouin zone. Euler angles (α, β, γ) relating the EFG and nuclear magnetic shielding tensor principal axis systems were determined using a modified version of the program EFG-Shield.[65] The definitions of these angles may also be found in ref 65. The quadrupole moment used to convert the largest component of the EFG tensor to the ^{43}Ca quadrupolar coupling constant was adjusted from the value of -4.09 fm^2 used by CASTEP to the recommended value of -4.08 fm^2.[7] Note that the structure representations in Figures 1 and 2 are to emphasize the different calcium coordination geometries; in fact all calculations in CASTEP are run using a unit cell as the input rather than an isolated molecule. Some localized orbital-based calculations were performed on calcite using Gaussian 03[66] to assess the improvement obtained through the plane-wave approach. During the course of our calculations, we noticed that the sign of the EFG tensor resulting from CASTEP calculations is opposite to the conventional definition but consistent with the sign used in Gaussian 03 calculations. That is, for both programs, the sign of the EFG must be reversed in order to compute the quadrupolar coupling constants according to $C_Q = eV_{33}Q/h$. The quadrupolar coupling constants reported by CASTEP incorporate this sign correction automatically. This can be readily verified by comparing the calculated values of the EFG and of C_Q for nuclei in diatomic molecules with the values available from high-resolution gas-phase microwave or molecular beam spectroscopy.[67] For example, we verified the sign of the oxygen-17 quadrupolar coupling constant for carbon monoxide, which is $+4.3205(7)$ MHz experimentally[68] and $+4.412$ MHz (GGA/PBE; 500 eV cutoff energy; default k-points; $10 \times 10 \times 10$ Å cell) according to our
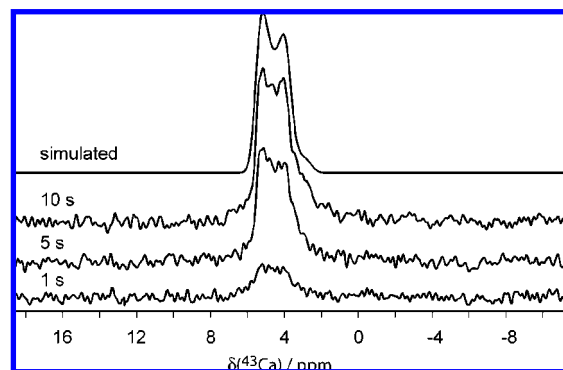

Figure 3. Natural abundance calcium-43 MAS NMR spectra of solid, powdered calcium carbonate (calcite polymorph, powdered single crystal sample) collected with different recycle delays. Each spectrum is the sum of 5k scans with a MAS rate of 3220 Hz.

GIPAW calculations. Carbon-13 magnetic shielding constants and chemical shifts were interconverted using the scale of Jameson and Jameson.[69]

Results and Discussion

1. Solid-State ^{43}Ca NMR Spectroscopy. Presented in Figure 3 are natural-abundance ^{43}Ca SSNMR spectra of powdered calcite obtained in a magnetic field of 21.1 T with magic-angle spinning. The series of spectra demonstrates that long recycle delays (several seconds or longer) are required to obtain good signal-to-noise for many calcium spectra; this is in contrast to many other quadrupolar nuclei with larger quadrupole moments. Previous work by Dupree and co-workers reported a ^{43}Ca MAS NMR spectrum of calcite at 8.45 T;[11] at that field strength, sufficient second-order quadrupolar broadening of the central transition was evident to enable a line shape simulation to extract the ^{43}Ca quadrupolar coupling constant (C_Q), asymmetry parameter (η_Q), and isotropic chemical shift (δ_{iso}). The values we obtained for C_Q and η_Q are in excellent agreement with the previous values (Table 1). We found, however, that our measured value of δ_{iso} (6 ± 2 ppm) was reproducibly slightly different from the previous report (14 ppm); we conclude that this is because of the nature of the saturated reference material.[34] For example, we observed that the chemical shift of 2 M $CaCl_2(aq)$ is -14 ± 2 ppm relative to a saturated solution; this is entirely consistent with the deshielding of the ^{43}Ca resonance observed previously as the concentration of aqueous calcium halide solutions was increased beyond 3.0 M.[70,71] We recorded ^{43}Ca MAS NMR spectra for several previously studied inorganic calcium compounds (see Supporting Information) and suggest solid calcium oxide as a reliable secondary reference material for future ^{43}Ca solid-state NMR studies. The resonance of CaO is sharp (the full-width at half-height is 22 Hz @ 21.1 T with MAS) and can be seen in a few scans with a 30 s recycle delay. We find the chemical shift of CaO(s) relative to that of saturated $CaCl_2(aq)$ is 120.4 ppm. This differs significantly from the previously reported value of 128 ppm,[11] thereby highlighting the problems associated with using $CaCl_2(aq)$ as a reference material.

(61) Koopmans, H. J. A.; van de Velde, G. M. H.; Gellings, P. J. *Acta Crystallogr.* **1983**, *C39*, 1323–1325.
(62) Burger, N.; Fuess, H.; Mason, S. A. *Acta Crystallogr.* **1977**, *B33*, 1968–1970.
(63) Medeiros, S. K.; Albuquerque, E. L.; Maia, F. F., Jr.; Caetano, E. W. S.; Freire, V. N. *Chem. Phys. Lett.* **2007**, *435*, 59–64.
(64) (a) Perdew, J. P.; Burke, K.; Ernzerhof, M. *Phys. Rev. Lett.* **1996**, *77*, 3865–3868. (b) Perdew, J. P.; Burke, K.; Ernzerhof, M. *Phys. Rev. Lett.* **1997**, *78*, 1396.
(65) Adiga, S.; Aebi, D.; Bryce, D. L. *Can. J. Chem.* **2007**, *85*, 496–505.
(66) Frisch, M. J. et al. *Gaussian 03, Revisions B.04 and C.02*; Gaussian, Inc., Wallingford, CT, 2004.
(67) Bryce, D. L.; Wasylishen, R. E. *Acc. Chem. Res.* **2003**, *36*, 327–334.
(68) Cazzoli, G.; Dore, L.; Puzzarini, C.; Beninati, S. *Phys. Chem. Chem. Phys.* **2002**, *4*, 3575–3577.

(69) Jameson, A. K.; Jameson, C. J. *Chem. Phys. Lett.* **1987**, *134*, 461–466.
(70) Farmer, R. M.; Popov, A. I. *Inorg. Nucl. Chem. Lett.* **1981**, *17*, 51–56.
(71) Lutz, O.; Schwenk, A.; Uhl, A. *Z. Naturforsch.* **1975**, *30a*, 1122–1127.

Table 1. Experimental ^{43}Ca Quadrupolar and Chemical Shift Tensor Data for the Calcite, Vaterite, and Aragonite Polymorphs of Calcium Carbonate[a]

	δ_{iso}, ppm	Ω, ppm	κ	C_Q, MHz	η_Q	α, deg	β, deg	γ, deg	reference
calcite	6 ± 2	8 ± 2	0.9 ± 0.1	1.39 ± 0.10	<0.05	0^b	0 ± 5	0^b	this work
	14	n/a	n/a	1.40	0.0	n/a	n/a	n/a	Dupree et al.[11]
vaterite	-3 ± 2	70 ± 20	0.0 ± 0.5	3.7 ± 0.5	0.55 ± 0.10	0 ± 20	30 ± 20	120 ± 20	this work[c]
aragonite	-34 ± 2	57 ± 4	0.23^d	<0.68	n/a	n/a	n/a	n/a	Dupree et al.[11]

[a] The isotropic chemical shift is defined as the average of the three CS tensor eigenvalues, $\delta_{iso} = (\delta_{11} + \delta_{22} + \delta_{33})/3$, and these are ordered as $\delta_{11} \geq \delta_{22} \geq \delta_{33}$. The span, Ω, is equal to $\delta_{11} - \delta_{33}$. The skew, κ, is equal to $3(\delta_{22} - \delta_{iso})/\Omega$. The quadrupolar asymmetry parameter, η_Q, is equal to $(V_{11} - V_{22})/V_{33}$ where the eigenvalues of the EFG tensor are ordered as follows: $|V_{33}| \geq |V_{22}| \geq |V_{11}|$. [b] Set to zero; however, these angles will not affect the spectrum in the present case where the EFG and CS tensors approach axial symmetry and the angle $\beta = 0$. [c] Because of the poor signal-to-noise of the ^{43}Ca SSNMR spectrum of static powdered vaterite, one must be aware that the Euler angles reported here may represent only one possible fit. [d] This has been corrected from the value of $\kappa = -0.07$ reported in the original reference.
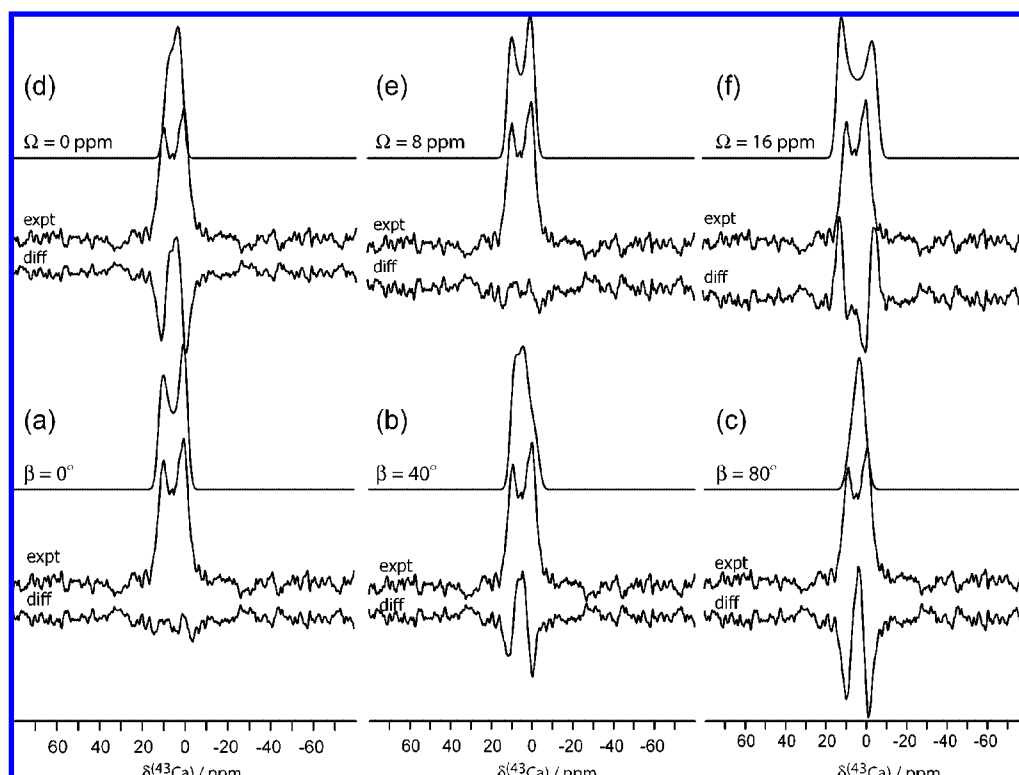

Figure 4. Experimental ^{43}Ca NMR spectrum of stationary calcite at 21.1 T. (a−c) Effect of varying the Euler angle β, which defines the angle between the largest component of the calcium electric field gradient tensor (V_{33}) and the δ_{33} component of the calcium CS tensor, on the simulated NMR spectrum. The difference spectra are also shown in each case; the best fit is obtained for $\beta = 0°$. All other parameters are kept constant at the values reported in Table 1. (d−f) Effect of varying the span of the calcium chemical shift tensor on the simulated ^{43}Ca NMR spectrum of stationary calcite at 21.1 T. The difference spectra are also shown in each case; the best fit is obtained for $\Omega = 8$ ppm. All other parameters are kept constant at the values reported in Table 1. Further simulations are reported in the Supporting Information.

The ^{43}Ca NMR spectrum of stationary powdered calcite at 21.1 T is shown in Figure 4. Calcite crystallizes in the $R\overline{3}c$ space group, and each calcium atom sits at a site of S_6 symmetry (Figure 1).[72] There is one magnetically unique calcium atom in the unit cell. As outlined by Robert and Wiesenfeld, S_6 symmetry requires that the symmetric part of the calcium magnetic shielding tensor have only two independent eigenvalues, which implies axial symmetry.[73] The axial symmetry ($\eta_Q = 0$) observed for the ^{43}Ca EFG tensor is also consistent with S_6 symmetry. The tensor orientations are restricted such that the eigenvectors corresponding to the unique eigenvalues of each tensor lie along the S_6 rotation axis. Simulation of the ^{43}Ca NMR spectrum obtained in this high magnetic field was

not possible without including an anisotropic chemical shift term in the simulation. Fortunately, because of the symmetry discussed above, the parameter space to be searched is greatly narrowed: we know that the skew of the CS tensor must be ± 1 and that the Euler angle β (describing the angle between the most shielded component of the CS tensor and the largest component of the EFG tensor, δ_{33} and V_{33}) must be $0°$ or $90°$. Spectral simulations shown in Figure 4 (angle β) and in the Supporting Information (skew) clearly indicate that $\beta = 0°$ and $\kappa = +1.0$. All that remains is to determine the span of the CS tensor; a systematic search yields a value for Ω of 8 ± 2 ppm (Figure 4 and Supporting Information). The effect of ignoring the calcium CSA completely is also shown in Figure 4. To verify the results obtained at 21.1 T (Table 1), we also acquired a ^{43}Ca NMR spectrum of powdered calcite at 11.75 T in order to ensure that the quadrupolar and CS tensor parameters were

(72) Markgraf, S. A.; Reeder, R. J. Am. Mineral. 1985, 70, 590–600.
(73) Robert, J. B.; Wiesenfeld, L. Phys. Rep. 1982, 86, 363–401.

indeed able to reproduce the ^{43}Ca NMR spectrum at more than one applied magnetic field strength (see Supporting Information).

Because of the high symmetry of calcite and the concomitant axial symmetry of the tensors, the results obtained through arguments described above also allow us to conclude that δ_{33} must lie along the 6-fold improper rotation axis, with the other two components of the tensor lying in the plane perpendicular to this. The absolute orientation of the EFG tensor in the molecular framework can be inferred without experiments (because it is traceless), i.e., V_{33} must lie along the 6-fold improper rotation axis. Since the relative orientation of the two tensors has been obtained experimentally, information has therefore been obtained on the *absolute* orientation of the CS tensor in the molecular frame without recourse to single-crystal NMR.

To our knowledge, this represents only the second published report of calcium CS anisotropy, the first being for the aragonite polymorph of $CaCO_3$.[11] However, no information on the relative orientation of the CS and EFG tensors was reported for aragonite. The results for calcite therefore represent the first full characterization of a calcium site by NMR in terms of the calcium-43 quadrupolar and CS tensor eigenvalues *and* the orientations of these tensors (relative and absolute). This was not possible previously for aragonite because of the dominance of the ^{43}Ca CS anisotropy ($\Omega = 57$ ppm) over the small quadrupolar interaction ($C_Q < 0.68$ MHz). The span of 8 ppm obtained for calcite is interesting in that it demonstrates that such small anisotropies may be characterized in ultrahigh magnetic fields for ^{43}Ca; however, on the basis of the known range of isotropic chemical shifts for calcium,[34] it is reasonable to expect that much larger spans may be observed (*vide infra*).

The value of Ω obtained for calcite allows for a direct comparison between ^{43}Ca CS tensors for two different polymorphic forms of calcium carbonate. Aragonite crystallizes in the *Pmcn* space group and has one magnetically unique calcium atom in the unit cell. The local symmetry at calcium in aragonite is C_s, and therefore the nuclear magnetic shielding tensor will have up to three unique eigenvalues.[73] The only restriction on tensor orientation is that one of the eigenvectors must be perpendicular to the mirror plane which passes through calcium. The symmetry restrictions on the tensors are seen in the results of DFT calculations (*vide infra*). More specifically, the nine-coordinate geometry of aragonite is best described as a distorted hula-hoop structure (Figure 1).[74] Point charge calculations[75] using the experimental calcite and aragonite structures reproduce the experimental observation that the magnitude of $C_Q(^{43}Ca)$ for calcite (6-coord) is roughly double that of aragonite (9-coord); we obtain a ratio of 1.61:1.00 using point charges. The small C_Q for aragonite compared to calcite is thus easily rationalized through this point charge model. The large CS tensor span for aragonite compared to calcite may be rationalized by considering that the CS anisotropy will collapse to zero in the case of a perfect octahedron (which is close to the case for calcite) whereas the distorted hula-hoop geometry about Ca in aragonite does not approach the requirement for an isotropic CS tensor (i.e., the idealized hula-hoop structure does not result in zero anisotropy).

2. Solid-State Calculations of ^{43}Ca Nuclear Magnetic Shielding and Quadrupolar Tensors. Given the extended ionic structure of calcite, we did not anticipate a good reproduction

of the experimental SSNMR parameters using a localized orbital-based computational approach. Our previous study of localized orbital calculations compared with GIPAW calculations of chlorine NMR parameters for alkaline earth chlorides indeed demonstrated the difficulties associated with the former approach.[65] Presently in the case of calcite, we find fair agreement between experiment and theory for a series of orbital-based calculations of the ^{43}Ca quadrupolar coupling constant (Figure 5a). However, the convergence with respect to basis set for the calcium shielding tensor is not ideal and was often much worse for other small ionic calcium compounds (data not shown). We instead pursued the calculation of the calcium quadrupolar and shielding tensor parameters for a series of small molecules using the GIPAW approach, where the extended nature of solids is taken into account through the use of plane-wave basis sets.[51,52] The robustness of this type of calculation with respect to plane-wave cutoff energy (analogous to basis set size) for calcite is also depicted in Figure 5; both $C_Q(^{43}Ca)$ and the shielding tensor eigenvalues are remarkably stable with respect to cutoff energy.

Shown in Figure 6 is the correlation obtained between calculated isotropic ^{43}Ca shielding constants and available ^{43}Ca isotropic chemical shifts measured previously[11,21,22] in the solid state for a series of small molecules. The correlation is described by $\sigma(\text{calc}) = -1.245 \times \delta(\text{expt}) + 1122.5$ ppm, and a correlation coefficient of $R = 0.983$. A similar deviation from a slope of unity when comparing experimental and calculated chemical shifts using the GIPAW approach has been noted previously for ^{35}Cl[76] and therefore does not seem to be a specific problem associated with calcium NMR parameters. The fact that there is a very good correlation between the experimental and calculated parameters suggests that the calculations may be useful in refining structural models using NMR data as restraints (*vide infra*). The correlation also suggests an effective absolute shielding constant for ^{43}Ca in saturated $CaCl_2$(aq) of 1122.5 ppm, which may again be potentially useful when using calculations in combination with NMR data to refine structural features.

Importantly, the calculations reproduce very well the only two known CS tensor spans, for calcite and aragonite (Table 2). The calculated values of 10.8 and 52.2 ppm, respectively, are practically within error of the experimental values, 8 ± 2 and 57 ± 4 ppm. In agreement with the symmetry rules of Robert and Wiesenfeld,[73] the calculations also correctly indicate axial symmetry of the ^{43}Ca shielding tensor in calcite (and produce the predicted number of antisymmetric components, one for both polymorphs). The coincidence of V_{33} and δ_{33} in calcite (as was observed experimentally) is also correctly calculated. Additionally, calculations for the other small molecules shown in Table 2 suggest that ^{43}Ca CS anisotropies should be readily measurable in many of these compounds; for example, the calculated span in calcium hydroxide is 39.6 ppm and that in $CaZrO_3$ is 64.3 ppm. By extension, we speculate that the ^{43}Ca CS tensor should be readily measureable in a wide variety of compounds and may be a useful additional tool in characterizing calcium binding sites.

Available values of $C_Q(^{43}Ca)$ are also well-reproduced by the calculations. For instance, the experimental data for calcite and aragonite are 1.39 ± 0.10 and <0.68 MHz, respectively, while the calculated values are 1.47 and 0.32 MHz. Certainly the

(74) Ruiz-Martínez, A.; Casanova, D.; Alvarez, S. *Chem. Eur. J.* **2008**, *14*, 1291–1303.

(75) Slichter, C. P. ; *Principles of Magnetic Resonance*, 3rd ed.; Springer-Verlag: Berlin, 1990; Section 10.6.

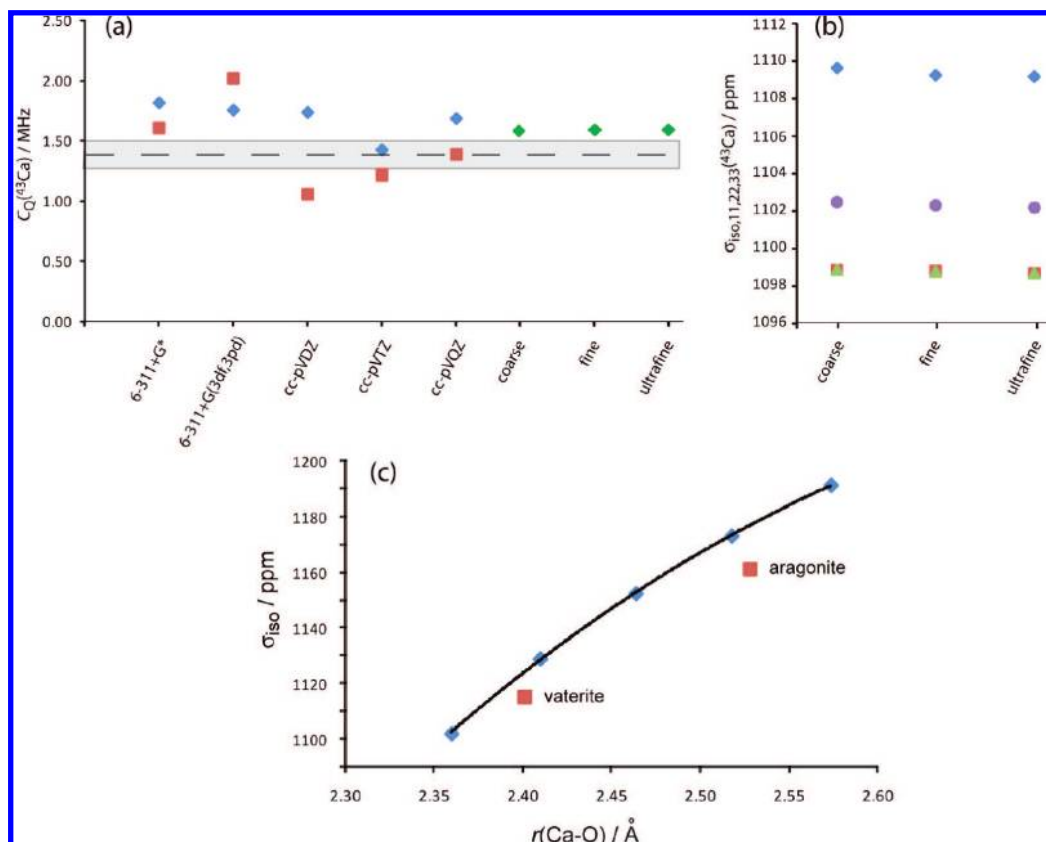(76) Bryce, D. L.; Bultz, E. B. *Chem. Eur. J.* **2007**, *13*, 4786–4796.

Figure 5. Comparison of selected results of quantum chemical calculations of calcium-43 NMR parameters for calcite. (a) Calculated [43]Ca quadrupolar coupling constants as a function of localized basis set (G03 calculations, red squares: RHF; blue diamonds: B3LYP; structural model shown in the Supporting Information) and as function of plane-wave cutoff energy (GIPAW calculations, green diamonds; coarse = 450 eV, fine = 550 eV, ultrafine = 610 eV). The experimental value of 1.39 MHz is denoted by a dashed line, and the error of 0.10 MHz is denoted by the shaded area. (b) GIPAW-calculated eigenvalues of the calcium nuclear magnetic shielding tensor (blue diamonds: σ_{33}; red squares: σ_{22}; green triangles: σ_{11}), and the isotropic value (purple circles: σ_{iso}), as a function of plane-wave cutoff energy. (c) GIPAW-calculated isotropic [43]Ca shielding constant as a function of the Ca–O distance (blue diamonds and trendline) in calcite. The experimental calcite structure was used ($r = 2.353$ Å) for the first data point, and in subsequent calculations all six Ca–O bond lengths were simultaneously increased (along with the length of the unit cell in the c direction). The line of best fit is $\sigma_{iso}/\text{ppm} = -631.9r^2 + 3531r - 3711$; $R^2 = 0.999$). The calculated shielding constants for aragonite and vaterite are shown as red squares; for these the average Ca–O distance is used for the x-coordinate.

calculations are successful in convincingly discriminating between the two polymorphs. Reasonable agreement is also obtained for CaZrO$_3$, for which an experimental value of 2.80 $\pm$ 0.03 MHz[21] may be compared to the calculated value of 2.30 MHz; however, this result demonstrates that agreement within experimental error cannot always be expected. The experimental values of C_Q and η_Q for calcium formate,[22] 1.24 $\pm$ 0.10 MHz and 0.90 $\pm$ 0.05, are presently calculated to be 1.24 MHz and 1.00, respectively. Most other calcium compounds which have been analyzed to date by [43]Ca SSNMR have yielded only line widths and not well-defined second-order quadrupolar line shapes due primarily to the small quadrupole moment of [43]Ca. Nevertheless, the present results suggest that plane-wave calculations will be useful for calculating calcium EFG tensors in addition to the above-mentioned magnetic shielding tensors. Interestingly, for the few values of C_Q discussed here, the 10–20% overestimation by GIPAW calculations observed previously for e.g., chlorine-35[76,77] and oxygen-17[77] quadrupolar coupling constants, is not seen for calcium.

3. Application of [43]Ca SSNMR and Solid-State Calculations To Provide Insight into the Structure of Vaterite. Vaterite is a metastable polymorph of calcium carbonate which has not been studied previously by [43]Ca SSNMR spectroscopy. As mentioned, there is debate over how to best describe the structure in a crystallographic space group, with
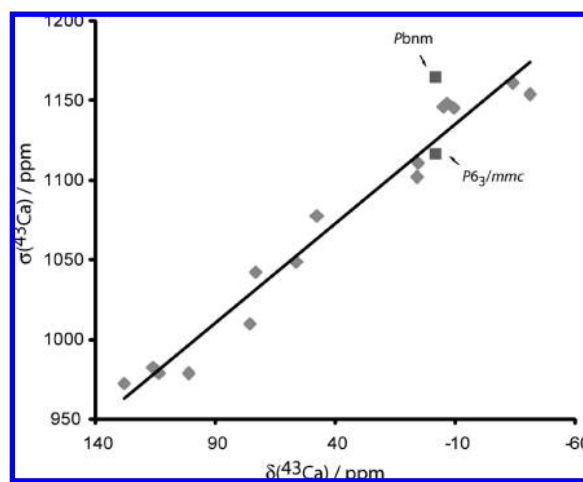

Figure 6. Correlation between calculated [43]Ca isotropic shielding constants (y axis) and experimental [43]Ca isotropic chemical shifts (x axis) for various calcium-containing compounds. The line of best fit is given by $\sigma(\text{calc}) = -1.245 \times \delta(\text{expt}) + 1122.5$ ppm with a correlation coefficient R of 0.983. Computed shielding constants are from Table 2. Experimental data are for CaB$_6$, CaBr$_2$, CaCl$_2$, CaF$_2$, Ca(OH)$_2$, CaS, CaSe, CaH$_2$, calcite, aragonite, CaMoO$_4$, CaO, CaWO$_4$, CaZrO$_3$, and calcium formate and are from refs 11, 21, and 22. The data points representing the vaterite *Pbnm* and *P6$_3$/mmc* structures were *not* included in the fit.

Table 2. GIPAW-Calculated ^{43}Ca Quadrupolar and Nuclear Magnetic Shielding Tensor Data for Various Compounds[a,b]

compound	σ_{iso}, ppm	σ_{11}, ppm	σ_{22}, ppm	σ_{33}, ppm	Ω, ppm	κ	C_Q, MHz	η_Q	α, deg	β, deg	γ, deg
CaCO$_3$ (calcite)	1102.1	1098.5	1098.5	1109.2	10.8	1.00	1.47	0.00	0.0	0.0	0.0
CaCO$_3$ (aragonite)	1161.2	1139.3	1152.7	1191.5	52.2	0.49	0.32	0.58	0.0	15.0	90.0
Ca(OH)$_2$	1042.6	1016.2	1055.8	1055.8	39.6	−1.00	−2.10	0.00	29.8	90.0	0.0
CaO	972.6	972.6	972.6	972.6	0.0	n/a	0.00	n/a	n/a	n/a	n/a
CaS	982.9	982.9	982.9	982.9	0.0	n/a	0.00	n/a	n/a	n/a	n/a
CaSe	978.9	978.9	978.9	978.9	0.0	n/a	0.00	n/a	n/a	n/a	n/a
CaH$_2$	978.8	963.6	973.9	998.9	35.3	0.42	0.87	0.87	90.0	13.7	0.0
CaF$_2$	1145.7	1145.7	1145.7	1145.7	0.0	n/a	0.00	n/a	n/a	n/a	n/a
CaCl$_2$	1048.9	1020.4	1053.1	1073.1	52.7	−0.24	−0.97	0.57	90.0	90.0	0.0
CaBr$_2$	1010.0	988.9	1018.5	1022.6	33.7	−0.76	−0.40	0.76	0.0	90.0	0.0
CaB$_6$	1153.9	1153.9	1153.9	1153.9	0.0	n/a	0.0	n/a	n/a	n/a	n/a
CaWO$_4$	1146.1	1142.9	1142.9	1152.4	9.4	1.00	1.36	0.00	140.2	0.0	0.0
CaMoO$_4$	1148.3	1145.3	1145.3	1154.4	9.1	1.00	1.16	0.00	142.8	0.0	0.0
CaZrO$_3$	1077.7	1056.1	1056.5	1120.4	64.3	1.00	2.30	0.15	0.0	10.5	90.0
Ca(HCOO$^-$)$_2$	1110.9	1093.2	1114.5	1125.2	32.0	−0.33	1.24	1.00	68.0	25.3	93.1

[a] All results were obtained with a planewave cutoff energy of 610 eV. See Experimental and Computational Details for further details. [b] The isotropic magnetic shielding constant, σ_{iso}, is equal to $(1/3)(\sigma_{11} + \sigma_{22} + \sigma_{33})$ where the eigenvalues of the shielding tensor are ordered as follows: $\sigma_{11} \leq \sigma_{22} \leq \sigma_{33}$. $\Omega = \sigma_{33} - \sigma_{11}$. $\kappa = 3(\sigma_{iso} - \sigma_{22})/\Omega$.

hexagonal ($P6_3/mmc$) and orthorhombic ($Pbnm$) structures both having been suggested.[48–50] The hexagonal structure exhibits static carbonate disorder about a pseudo 6-fold axis. The orthorhombic structure features 8-fold coordination at calcium (eight oxygens at 2.6 Å or less; see Figure 2) while the hexagonal structure exhibits 6-fold coordination (six oxygens at 2.6 Å or less with two more oxygens at 2.9 Å). Recently, Medeiros et al. proposed two DFT-refined versions of the orthorhombic representation (one calculated using the local density approximation (LDA) and the other with the generalized gradient approximation (GGA)).[63] They conclude that more work is needed to determine the best representation of the vaterite polymorph; in particular they did not analyze the hexagonal representation in their study. On the basis of the success we have obtained in analyzing ^{43}Ca SSNMR spectra of calcite and the excellent agreement between experimental and calculated calcium NMR parameters (*vide supra*), we now have a validated strategy to probe the structure of vaterite.

Depicted in Figure 7(d) is the experimental ^{43}Ca MAS NMR spectrum of vaterite along with a simulated spectrum based on the parameters given in Table 1. A relatively large value of C_Q is obtained, 3.7 ± 0.5 MHz, and the chemical shift of $−3 \pm 2$ ppm is intermediate compared with the other two CaCO$_3$ polymorphs. The large error in the value of C_Q is a result of the relatively featureless line shape and accounts for a distribution of values possibly due to disorder. It is somewhat surprising that such a large quadrupolar interaction would not give a more well-defined line shape; we take this as a first possible indication of static disorder in vaterite which would be consistent with the hexagonal structure.

Previously, a correlation of 280 ppm Å^{-1} between the isotropic ^{43}Ca chemical shift and the mean Ca–O distance was proposed on the basis of data obtained for 12 inorganic calcium compounds.[11] A more detailed experimental and theoretical demonstration of the dependence of shielding constants on internuclear distance in solids has been presented by de Dios et al. in the case of ^{87}Rb shifts of cubic rubidium halides, with the shielding constant increasing with increasing internuclear distance.[78] Recent ^{43}Ca NMR data also seem to fit with this trend;[21,22] however, Wong et al. noted a deviation from the trend

for CaZrO$_3$.[22] Our experimental results for vaterite seem to fit with the trend. If we examine the three polymorphs of CaCO$_3$, for example, the mean Ca–O distances are 2.353, 2.528, and 2.401 Å ($P6_3/mmc$ structure, including oxygens at less than 2.6 Å) for calcite, aragonite, and vaterite, respectively, while their chemical shifts are 6, −34, and −3 ppm, respectively. To test the hypothesis that the chemical shift is strongly correlated to the average Ca–O bond length, we calculated the value of $\sigma_{iso}(^{43}$Ca$)$ as a function of Ca–O distance, using the calcite structure as a starting point (Figure 5(c)). Also shown in the figure are the relevant data for aragonite, which demonstrates that despite the differences in coordination number and geometry between calcite and aragonite, the shielding constant for aragonite may be reproduced quite well taking only the Ca–O bond length into account.

The ^{43}Ca NMR spectrum of a stationary sample of vaterite acquired at 21.1 T is presented in Figure 8, along with a simulated spectrum based on the experimental parameters given in Table 3. While the spectrum suffers from low signal-to-noise (we suspect due to the long longitudinal relaxation time constant), it is clear that there is a significant contribution from calcium CS anisotropy. Large errors reported in Table 3 are a consequence of the low signal-to-noise. The value obtained for the span, 70 ± 20 ppm, is the largest known to date for calcium. This value is clearly significantly different from that measured for calcite (8 ± 2) and therefore further suggests the utility of calcium CS tensors in distinguishing between polymorphs. This could become useful since in high magnetic fields many calcium-43 MAS NMR spectra are featureless lines, and it is difficult to obtain precise quadrupolar coupling constants. The values of $\Omega(^{43}$Ca$)$ are comparable to values of Ω obtained for other group 2 nuclei. For example, values ranging from 3 to 65 ppm have been obtained experimentally for ^{9}Be, in Be(acac)$_2$ and bis(cyclopentadienyl)beryllium, respectively.[79,80] For ^{25}Mg, the CSA has typically been too small to detect experimentally; however, computational estimates for bis(pyridine)(5,10,15,20-tetraphenylporphyrinato)magnesium(II) and related compounds

(77) Gervais, C.; Dupree, R.; Pike, K. J.; Bonhomme, C.; Profeta, M.; Pickard, C. J.; Mauri, F. *J. Phys. Chem. A* **2005**, *109*, 6960–6969.

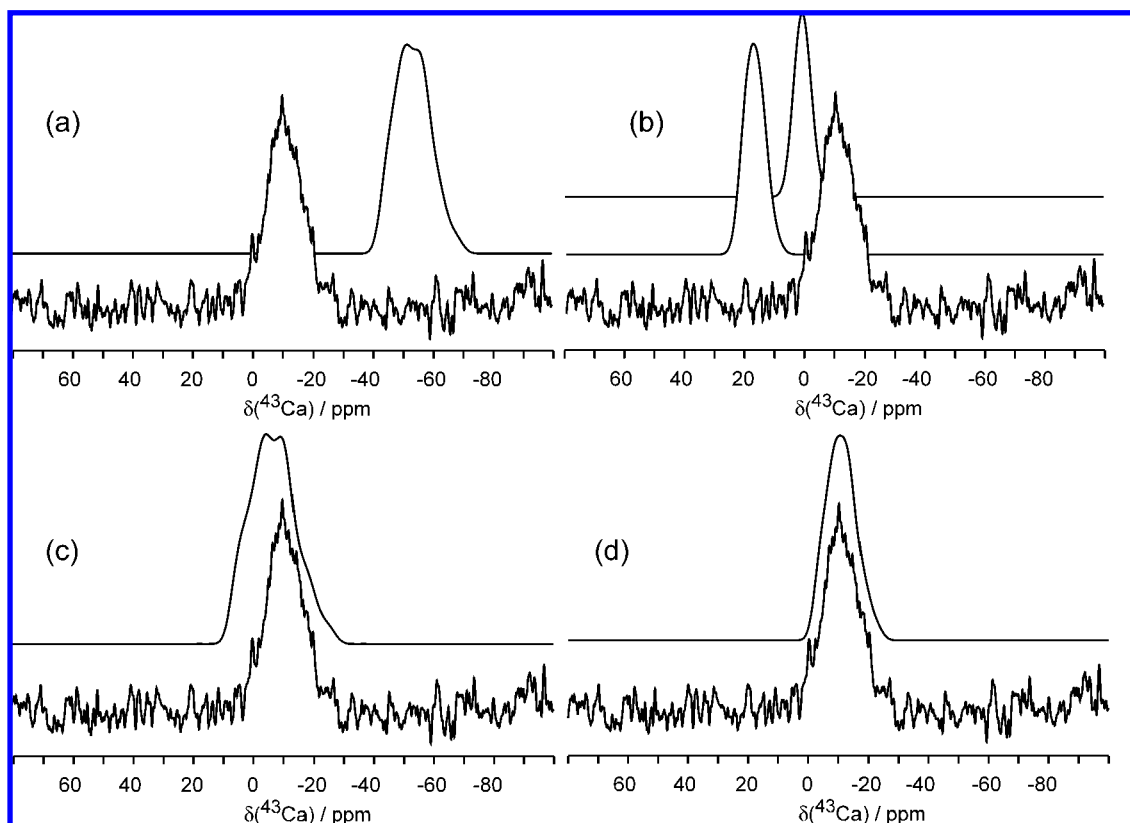(78) de Dios, A. C.; Walling, A.; Cameron, I.; Ratcliffe, C. I.; Ripmeester, J. A. *J. Phys. Chem. A* **2000**, *104*, 908–914.

(79) Bryce, D. L.; Wasylishen, R. E. *J. Phys. Chem. A* **1999**, *103*, 7364–7372.

(80) Hung, I.; Macdonald, C. L. B.; Schurko, R. W. *Chem. Eur. J.* **2004**, *10*, 5923–5935.

Figure 7. Experimental and simulated ^{43}Ca MAS NMR spectra of the vaterite polymorph of $CaCO_3$ acquired at 21.1 T. The experimental spectrum, shown in the lower trace of each part, is the sum of 4790 scans with a recycle delay of 20 s. The MAS rate was 5 kHz. The spectra shown in the upper trace of each part have been simulated using the NMR parameters calculated using CASTEP for the following structural models of vaterite: (a) *Pbnm*; (b) LDA-ortho (middle trace) and GGA-ortho (upper trace); (c) hexagonal *P6$_3$/mmc*; (d) best-fit simulation. Gaussian broadening of 300 Hz is applied to each simulated spectrum.
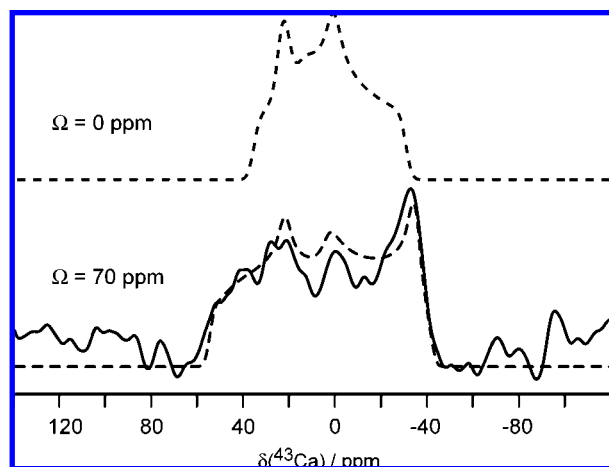

Figure 8. Experimental and simulated ^{43}Ca NMR spectra of a powder sample of the vaterite polymorph of calcium carbonate under stationary conditions. The experimental spectrum (solid line) is the sum of 7k scans with a recycle delay of 20 s, acquired at 21.1 T. The upper dashed line is a simulation based only on the ^{43}Ca quadrupolar parameters obtained from the MAS NMR spectrum and ignores calcium chemical shift anisotropy. The lower dashed trace represents the fit to the experimental spectrum, for which $\Omega = 70$ ppm. Other parameters are given in Table 3.

are less than 60 ppm[81,82] and for bis(cyclopentadienyl)magnesium the CSA is calculated to be 40–50 ppm.[83] Thus, at present the available values of Ω for group 2 nuclei are consistently quite small.

We next applied the GIPAW method to calculate the ^{43}Ca quadrupolar and nuclear magnetic shielding tensors for four possible vaterite structures: orthorhombic *Pbnm*, LDA-ortho, GGA-ortho, and hexagonal *P6$_3$/mmc*. The results, summarized in Table 3, do not immediately overwhelmingly favor one of the structures when these results are compared to experiment. However, further examination of the data suggests that the hexagonal structure provides calculated results which are more consistent with the experimental ^{43}Ca NMR data. This is easily illustrated by generating simulated ^{43}Ca MAS NMR spectra using the calculated parameters and then comparing these spectra to the experimental one (Figure 7a–c). Clearly the *Pbnm* structure results in a chemical shift which is far too low compared to experiment. The LDA-ortho and GGA-ortho structures have chemical shifts which are closer to experiment, but the calculated quadrupolar coupling constants are much too small. The *P6$_3$/mmc* results provide the most convincing fit to the experimental MAS NMR spectrum when considering both the isotropic chemical shift and the quadrupolar parameters (e.g., η_Q is 0.55 ± 0.10 experimentally and calculated to be 0.56 on the basis of the *P6$_3$/mmc* structure). The improved fit to the previously established isotropic chemical shift correlation for the *P6$_3$/mmc* structure compared to the *Pbnm* structure is

(81) Wong, A.; Ida, R.; Mo, X.; Gan, Z.; Poh, J.; Wu, G. *J. Phys. Chem. A* **2006**, *110*, 10084–10090.
(82) Wu, G.; Wong, A.; Wang, S. *Can. J. Chem.* **2003**, *81*, 275–283.
(83) Hung, I.; Schurko, R. W. *Solid State Nucl. Magn. Reson.* **2003**, *24*, 78–93.

Table 3. GIPAW-Calculated ^{43}Ca Quadrupolar and Nuclear Magnetic Shielding Tensor Data for Various Proposed Structures of Vaterite[a]

	σ_{iso}, ppm	σ_{11}, ppm	σ_{22}, ppm	σ_{33}, ppm	Ω, ppm	κ	C_Q, MHz	η_Q	α, deg	β, deg	γ, deg
Pbnm	1164.7	1115.1	1175.1	1203.9	88.7	−0.35	3.91	0.50	63	27	104
LDA-ortho	1099.9	1053.0	1112.1	1134.6	81.6	−0.45	−2.81	0.43	61	88	0
GGA-ortho	1117.9	1086.3	1122.9	1144.3	58.0	−0.26	−2.27	0.65	86	83	173
P6₃/mmc	1115.1	1089.1	1089.5	1166.8	77.7	0.99	4.37	0.56	0	9	82
expt	1125.5 ± 1[b]	-	-	-	70 ± 20	0.0 ± 0.5	±(3.7 ± 0.5)	0.55 ± 0.10	0 ± 20	30 ± 20	120 ± 20

[a] See footnotes to Tables 1 and 2 for definitions of shielding and EFG parameters. [b] Converted from the experimental chemical shift using the value for σ_{ref} determined from Figure 6: $\delta = 1122.5$ ppm $- \sigma$. Using the full equation from Figure 6 results instead in a value of 1126.2 ± 1 ppm.

Table 4. GIPAW-Calculated ^{13}C Nuclear Magnetic Shielding Tensor Data for Various Proposed Structures of Vaterite[a]

	σ_{iso}, ppm	σ_{11}, ppm	σ_{22}, ppm	σ_{33}, ppm	Ω, ppm	κ
Pbnm	−4.1	−36.0	−23.2	46.9	82.8	0.69
LDA-ortho	23.5	−24.9	35.9	59.6	84.4	−0.44
GGA-ortho	−0.1	−28.0	−18.3	46.0	74.0	0.74
P6₃/mmc	11.7	−17.1	−3.2	55.0	72.0	0.61
expt[b]	14.3 ± 1.0	−17.1	−1.5	60.9	78 ± 5	0.6 ± 0.1

[a] See footnotes to Table 2 for definitions of shielding parameters. [b] Experimental chemical shift tensor eigenvalues were converted to the shielding eigenvalues shown here using the absolute shielding scale of Jameson and Jameson, $\delta = 184.1$ ppm $- \sigma$, where 184.1 ppm is the absolute ^{13}C shielding constant for tetramethylsilane (liquid, spherical bulb).

depicted in Figure 6. The calculated shielding constant for the *P6₃/mmc* structure also fits in with the trend depicted in Figure 5c. The calculated CS tensor spans for the orthorhombic and hexagonal structures, 88.7 and 77.7 ppm, respectively, do not strongly provide additional evidence for the *P6₃/mmc* structure because of the large error on the experimental value; however, the *Pbnm* value is much closer to the edge of the experimental range (*cf.* expt value of 70 ± 20 ppm). Simulated spectra of stationary vaterite based on the calculated parameters for the *Pbnm* and *P6₃/mmc* structures obviously do not exactly reproduce the experimental spectrum; however, the qualitative shape of the "*P6₃/mmc* spectrum" is arguably closer to the experimental line shape than is the line shape of the "*Pbnm* spectrum" (Supporting Information).

As a final check on the validity of the *P6₃/mmc* model for vaterite over the *Pbnm* model, we acquired and simulated ^{13}C SSNMR spectra (Supporting Information). Shielding tensor components for the various proposed structures are presented in Table 4. The span and skew of the ^{13}C shielding tensor for the *Pbnm* and *P6₃/mmc* structures unfortunately compare approximately equally well with experiment. However, the isotropic chemical shift for the hexagonal structure lies close to the experimental value while that for the orthorhombic structure is over 18 ppm away. Therefore the ^{13}C NMR data are also consistent with the conclusion that the hexagonal *P6₃/mmc* structure is the preferred representation for vaterite.

Conclusion

The present study has provided a complete interpretation of a calcium-43 SSNMR spectrum in terms of the quadrupolar and CS tensors, including their relative orientation. The characterization of the calcium CS tensor in calcite represents a milestone of sorts in that this compound was also the focus of Lauterbur's pioneering measurement of a ^{13}C CS tensor in 1958,[84] and was the first inorganic carbonate to be characterized by ^{17}O MAS

NMR by Smith in 1995.[85] Given the low quadrupole moment of ^{43}Ca and the requirement of high magnetic fields for studying limited amounts of sample at natural abundance in ^{43}Ca, the calcium CS tensor should often prove to be measureable since under such circumstances the second-order quadrupolar effects will be small, but the effects of CS anisotropy will be amplified. This will become increasingly important as commercially available magnetic field strengths continue to increase.

We have also shown that GIPAW calculations reproduce well the available calcium quadrupolar and CS tensor data, including tensor anisotropies. Significantly, our combined experimental and theoretical results suggest the utility of the calcium CS tensor as a novel probe of calcium binding environments in a range of calcium-containing materials. For example, for three polymorphs of the same compound we have found that the CS tensor span ranges from 8 to 70 ppm and demonstrated how the symmetry around calcium is reflected differently in the CS tensor as compared with the EFG tensor. An effective absolute shielding constant for ^{43}Ca in saturated $CaCl_2$(aq) of 1122.5 ppm is proposed. The experimental and theoretical methods were then applied in a case study to demonstrate the power of ^{43}Ca SSNMR in cross-validating X-ray crystallographic data. Although this was not an easy problem to sort out because of the very small differences between proposed structures, we have argued that a preponderance of the evidence obtained for vaterite allows us to conclude that its crystal structure is better described by the hexagonal *P6₃/mmc* space group rather than the orthorhombic *Pbnm*. The combination of ^{43}Ca SSNMR spectroscopy and GIPAW DFT calculations holds promise as a strategy for providing structural information which is complementary to that obtained through diffraction methods.

(84) Lauterbur, P. C. *Phys. Rev. Lett.* **1958**, *1*, 343–344.

(85) Smith, M. E.; Steuernagel, S.; Whitfield, H. G. *Solid State Nucl. Magn. Reson.* **1995**, *4*, 313–316.
(86) Brandenburg, K. Diamond, Version 3.0e, Crystal Impact GbR; Bonn, Germany, 1997−2005.
(87) Cason, C.; Froehlich, T.; Kopp, N.; Parker, R. POV-Ray for Windows, Version 3.6.1c.icl8.win32, 2006.

sity of Ottawa (www.nmr900.ca). NSERC is acknowledged for a Major Resources Support grant.

Supporting Information Available: Full ref 66; four tables reporting chemical shift and nuclear magnetic shielding tensor information according to different conventions; figures showing as follows: [43]Ca SSNMR spectra of CaO and other small molecules; ^{13}C SSNMR spectrum of vaterite; [43]Ca SSNMR spectrum of calcite at 11.75 T; powder X-ray diffraction pattern for vaterite; simulated [43]Ca SSNMR spectra for calcite which demonstrate the sensitivity of the fit to the CS tensor skew, span, and angle β; simulated [43]Ca SSNMR spectra based on GIPAW-calculated parameters for stationary vaterite; structural model used for localized orbital calculations on calcite. This material is available free of charge via the Internet at http://pubs.acs.org.

JA8017253